

1 **East European chironomid-based calibration model for past summer**  
2 **temperature reconstructions**

3

4 Tomi P. Luoto<sup>1,\*</sup>, Bartosz Kotrys<sup>2</sup> and Mateusz Płóciennik<sup>3</sup>

5

6 <sup>1</sup>Faculty of Biological and Environmental Sciences, Ecosystems and Environment Research

7 Programme, University of Helsinki, 15140 Lahti, Finland

8

9 <sup>2</sup>Polish Geological Institute - National Research Institute, Pomeranian Branch in Szczecin, 71-130

10 Szczecin, Poland

11

12 <sup>3</sup>Department of Invertebrate Zoology and Hydrobiology, Faculty of Biology and Environmental

13 Protection, University of Lodz, 90-237 Lodz, Poland

14

15 \*Corresponding author (e-mail: [tomi.luoto@helsinki.fi](mailto:tomi.luoto@helsinki.fi))

16

17

18

19

20

21

22

23

24

25 *Running page head: East European chironomid-temperature model*

26 ABSTRACT: Understanding local patterns and large scale processes in past climate necessitates  
27 detailed network of temperature reconstructions. In this study, a merged temperature inference  
28 model using fossil chironomid (Diptera: Chironomidae) datasets from Finland and Poland was  
29 constructed to fill the lack of an applicable training set for East European sites. The developed  
30 weighted averaging-partial least squares (WA-PLS) inference model showed favorable performance  
31 statistics suggesting that the model can be useful for downcore reconstructions. The combined  
32 calibration model includes 212 sites, 142 taxa and a temperature gradient of 11.3-20.1 °C. The 2-  
33 component WA-PLS model has a cross-validated coefficient of determination of 0.88 and a root  
34 mean squared prediction error of 0.88 °C. We tested the new East European temperature transfer  
35 function in chironomid stratigraphies from a Finnish high-resolution short-core sediment record and  
36 a Polish paleolake (Żabieniec) covering the past ~20,000 yr. In the Finnish site, the chironomid-  
37 inferred temperatures correlated closely with the observed instrumental temperatures showing  
38 improved accuracy compared to estimates by the original Finnish calibration model. In addition, the  
39 long-core reconstruction from the Polish site showed logical results in its general trends compared  
40 to existing knowledge on the past regional climate trends, however, with distinct differences when  
41 compared with hemispheric climate oscillations. Hence, based on these findings, the new  
42 temperature model will enable more detailed examination of long-term temperature variability in  
43 Eastern Europe, and consequently reliable identification of local and regional climate variability of  
44 the past.

45

46 KEYWORDS: Chironomidae, Climate reconstruction, Finland, Holocene, Late Glacial,  
47 Paleoclimate, Poland, Training set, Transfer function

48

49

50

51 **1. INTRODUCTION**

52

53 Advances in paleoclimatology have enabled building of comprehensive outline of climate  
54 changes of the recent past, the Holocene epoch and the last Glacial cycle (McCarroll 2015, Wanner  
55 et al. 2015, Linderholm et al. 2018). However, the local differences and small-scale variation are  
56 still poorly established in several geographic areas. In addition to high-fidelity sediment archives,  
57 the paleoclimatological toolpack needs to be refined to tackle reliably the climate variability of the  
58 past. Non-biting midges (Insecta: Diptera: Chironomidae) have been recognized as one of the most  
59 powerful proxies to reconstruct past summer air temperature dynamics (Brooks 2006). Utilizing the  
60 fossil community compositions of the temperature-sensitive chironomid taxa and applying the  
61 calibration set approach via a transfer function, quantitative climate inferences have become  
62 available from sites where other paleoclimate proxies have failed or are not possible to use  
63 (Ilyashuk et al. 2011, Luoto et al. 2018). In addition to confounding environmental variables, such  
64 as nutrients (Quinlan & Brodersen 2006, Eggermont & Heiri 2012, Medeiros et al. 2015), a  
65 potential downside of chironomids as a paleotemperature proxy lays in the suitability of the  
66 calibration set to the downcore site (Engels et al. 2014). In an ideal situation, the downcore site  
67 should be within the geographical area of the training set, the study site characteristics (such as lake  
68 size and depth) should be similar and the calibration sites should constitute a temperature gradient  
69 that covers the expected range of past temperature changes. When applying inference models to  
70 cores outside the training set's geographical or environmental range, problems related to taxa  
71 occurrences (poor modern analogues) and unrealistic taxon-specific temperature optima arises.  
72 Moreover, continental scale calibration sets (Heiri et al. 2011) may not be able to detect small-  
73 magnitude variation in temperatures, although they can be very useful in reconstructing the large-  
74 scale climate patterns.

75 Previously, it has been challenging to produce reliable chironomid-based temperature  
76 inferences at the ends of the temperature gradient in Eastern Europe. In downcore sites located in  
77 southern Finland, temperatures of the warm climate events, such as the recent warming, Medieval  
78 Climate Anomaly and Holocene Thermal Maximum, may have been underestimated due to lack of  
79 equally warm calibration sites (Rantala et al. 2016, Shala et al. 2017). Similarly, the lack of warm  
80 calibration sites in the available chironomid-based temperature inference models have thus far  
81 caused problems in downcore studies of Polish sites due to deficiency of warm analogues  
82 (Pawłowski et al. 2015, 2016a). Here, we combine the Finnish calibration sets (Luoto 2009, Luoto  
83 et al. 2016) with a dataset collected from Poland (previously unpublished) to create a more  
84 applicable temperature inference model for East European sites than has previously been available.  
85 In addition to standard numerical testing of the model performance, we validate the model using a  
86 chironomid stratigraphy from an annually laminated lake sediment record from Finland and  
87 compare the reconstruction against instrumentally measured temperatures. In addition, we apply the  
88 East European calibration model on a chironomid record from a Polish paleolake covering the past  
89 ~20,000 yr and compare the output against previous reconstructions. We aim to produce a new  
90 quantitative tool for more reliable reconstructions of past climate patterns in the East European  
91 sector to better describe local climate variability.

92

## 93 **2. MATERIAL AND METHODS**

94

### 95 **2. 1. Study sites and sediments**

96

97 The training set study sites comprise of 212 lakes located in Finland and Poland (Fig. 1).  
98 The 114 Finnish sites, collected with a Limnos gravity corer between 2005 and 2014, originate from  
99 two previously published datasets located at a treeline transect in northeastern Lapland (32 lakes,

100 68°47' – 69°55'N) (Luoto et al. 2016) and along the latitudinal gradient of Finland (82 lakes, 60°13'  
101 – 69°53'N) (Luoto 2009). The mean July air temperature in the Finnish sites varies between 11.3  
102 and 17.1 °C (mean 14.4 °C, median 14.1 °C) within an altitudinal gradient of 4-405 m a.s.l. All the  
103 sites are small and shallow (0.5-7.0 m) with pH between 4.6 and 8.4. The 98 Polish lakes, sampled  
104 in summer 2014 using a Kajak corer, are located between 49°19'–54°68'N and constitute an  
105 altitudinal gradient of 4-1624 m a.s.l. The mean July air temperature in the Polish sites varies  
106 between 11.6 and 20.1 °C (mean 18.6 °C, median 18.9 °C), whereas the depth range is 0.3-15.0 m.  
107 The lake water pH fluctuate between 5.1 and 9.8. The Polish dataset is previously unpublished.  
108 Comparison between the combined training sets is given in Table 1.

109         The short-core test site Lake Nurmijärvi (61°35'N, 25°55'E; 87.7 m a.s.l.) is located in  
110 south-central Finland (Fig. 1). The lake with annually laminated sediments is currently  
111 circumneutral (pH = 7.0) and mesotrophic. The mean July air temperature at the study site is 16.9  
112 °C (climate normals 1981–2010, Finnish Meteorological Institute). The sediment sequence was  
113 cored in winter 2016 using a HTH-corer and subsampled at 1-cm intervals. The average sample  
114 interval in the verified varve chronology (Ojala et al. 2016, 2018) is 4 years and the available  
115 meteorological data begins from the 1830s. The full chironomid stratigraphy of Nurmijärvi is  
116 published (Luoto & Ojala 2016).

117         The long-core sediment site Żabieniec (51°51'N; 19°46'E; 180 m a.s.l.) is currently a bog  
118 located in central Poland (Fig. 1). The present-day mean July air temperature at the study site is 18  
119 °C. Detailed descriptions of the study site and the paleolake sediments together with the full  
120 chironomid stratigraphy and chronology are given elsewhere (Płóciennik et al. 2011). In brief, the  
121 paleolake sediments were sampled using a piston corer and the subsampling was performed at  
122 varying intervals. The stratigraphy represents roughly the past 20,000 yr. The chronology of the  
123 core is based on 13 radiocarbon dates and the age-depth model is originally presented in  
124 Lamentowicz et al. (2009).

125

## 126 **2.2. Chironomid analysis**

127

128 Fossil chironomid analysis was performed using standard methods in all the datasets and  
129 cores applying provided guidelines (Brooks et al. 2007). In short, a 100 µm mesh was used for  
130 sieving at least 50 chironomid head capsules per sample. Similar to unidentified remains, other  
131 midges than chironomids were ignored. Taxonomic harmonization of the training sets and the two  
132 sediment downcores was achieved through close collaboration between the chironomid analysts.  
133 The morphologically similar taxa *Thienemanniola* and *Constempellina* were separated in the  
134 combined training set according to their contemporary occurrence described in species checklists  
135 (Paasivirta 2014, Sæther and Spies 2013). In some cases (including *Ablabesmyia*, *Dicrotendipes*  
136 and *Microtendipes*), species type-level identification was scaled to genus-level.

137

## 138 **2.3. Statistical analyses**

139

140 Taxon-specific mean July temperature optima in the merged dataset were estimated using  
141 Weighted Averaging (WA) with log<sub>10</sub> transformed species data in the program C2 version 1.7.2  
142 (Juggins 2007). Generalized Linear Modeling (GLM) was used to assess taxa that significantly ( $p \leq$   
143 0.05) respond to mean July air temperature. The GLMs were run using Poisson distribution in the  
144 program Past3 (Hammer 2001). Detrended Correspondence Analysis (DCA) was used to assess the  
145 gradient lengths of the first two DCA axis for selection of the most suitable methods for further  
146 analyses. For linearly distributed data with short gradient lengths, Principal Component Analysis  
147 (PCA) and redundancy analysis (RDA) are the most suitable methods (Šmilauer & Lepš 2014). The  
148 primary PCA axis scores were compared with site-specific temperatures using Pearson Product-  
149 moment correlation coefficient ( $R$ ), coefficient of determination ( $R^2$ ) and the level of statistical

150 significance ( $p < 0.05$ ) to verify that the communities are responding to temperature. In addition,  
151 RDA with forward-selected environmental variables and 999 unrestricted permutations was used to  
152 partial out the significance of temperature, depth and pH (variables available from all datasets) on  
153 the chironomid assemblages in the joint dataset. The DCA, PCA and RDA were performed with  
154 log<sub>10</sub> transformed species data using the CANOCO 5 program (Šmilauer & Lepš 2014).

155         The combined East European chironomid-based calibration model of mean July air  
156 temperature was developed using the Weighted Averaging - Partial Least Squares technique (WA-  
157 PLS), also with log<sub>10</sub> transformed species data. The number of useful regression calibration  
158 components was assessed using *t*-test (significance level 0.05). Model performance was evaluated  
159 using jackknife cross-validation and subsequent coefficient of determination ( $R^2_{\text{Jack}}$ ), root mean  
160 squared error of prediction (RMSEP) and mean and maximum biases. The model was constructed  
161 using the program C2 version 1.7.2 (Juggins 2007), in which also other common model types were  
162 initially tested.

163         The model was verified against instrumentally measured (meteorological) temperatures  
164 available since the 1830s in the shortcore sediment record from Nurmijärvi. The chironomid-  
165 inferred temperatures were tested against the observational data by applying  $R$ ,  $R^2$  and  $p < 0.05$ .  
166 Sample-specific modeling errors (estimated standard error of prediction = eSEP) were determined  
167 using bootstrapping cross-validation with 999 iterations. The model was also run to reconstruct  
168 temperatures in the Żabieniec long-core sediment record. LOESS smoothing was used to depict  
169 general trends using a span of 0.2. To test whether the Żabieniec reconstruction corresponded to the  
170 primary chironomid community variability, the temperatures were compared against the PCA axis 1  
171 scores using Pearson product-moment correlation coefficient and the associated level of statistical  
172 significance. Using the modern analogue technique, the cut-level of the 5<sup>th</sup> percentile of all squared-  
173 chord distances in the modern calibration data was determined. These distances were then compared  
174 to the distance between each fossil assemblage and its most similar assemblage in the modern data

175 set and used to define ‘no close’ analogues. The reconstruction was compared with previous  
176 chironomid-based reconstructions from the focal core using the Norwegian (Brooks & Birks 2001,  
177 unpubl.), Russian (Self et al. 2011) and Swiss (Heiri & Lotter 2005, Bigler et al. 2006, von Gunten  
178 et al. 2008) calibration models. In addition, the reconstructed general local trends in temperature  
179 were compared with an ice-core temperature record (site-specific calibrations using ice-isotopic  
180 ratios, borehole temperatures and gas-isotopic ratios) from Greenland (GISP2, Cuffey & Clow  
181 1997, Alley 2000) representing hemispheric climate development.

182

### 183 3. RESULTS

184

185 After merging the Finnish and Polish chironomid training sets, 142 taxa were encountered  
186 from the 212 calibration sites (Fig. 2). *Psectrocladius sordidellus*-type occurred in 86 sites,  
187 *Polypedilum nubeculosum*-type in 80 sites and *Dicrotendipes* and *Procladius* in 79 sites.  
188 *Limnophyes* reached the maximum relative abundance (75%) in a single site. *Lauterborniella*  
189 *agrayloides* (6.7%), *Ablabesmyia* (6.5%) and *Paratendipes nudisquama*-type (5.4%) had the  
190 highest mean abundances in the combined dataset.

191 The taxa with coldest temperature optima (12.5-13.1 °C) included *Heterotrissocladius*  
192 *maeaeri*-type, *Psectrocladius calcaratus*-type and *Zalutschia* type B, whereas the taxa having  
193 warmest optima included *Polypedilum sordens*-type, *Glyptotendipes barbipes*-type and *Labrundinia*  
194 *longipalpis* (18.8-18.9 °C) (Fig. 3). Taxa with intermediate temperature optima (16-17 °C) and wide  
195 tolerances included *Paratanytarsus penicillatus*-type, *Dicrotendipes*, *Procladius* and *Chironomus*  
196 *anthracinus*-type. Of the most common taxa (N > 5), only *Dicrotendipes* did not respond  
197 statistically significantly to the temperature gradient (Fig. 3). For most taxa, the GLMs showed  
198 significant linear fit, however, significant nonlinear distribution was found in some taxa with  
199 intermediate temperature optima, including *Tanytarsus chinyensis*-type 1, *Natarsia Punctata*-type,



200 *Corynoneura lobata*-type, *Smittia* and *Endochironomus impar*-type. *Paratanytarsus penicillatus*-  
201 type was the only taxon with bimodal distribution, with highest abundances at the both ends of the  
202 temperature gradient.

203 The initial DCA indicated a gradient length of 2.8 SD for the surface sediment chironomid  
204 assemblages. Hence, owing to the linear nature of the data, PCA was recommended for ordination  
205 analysis (Šmilauer and Lepš, 2014). Subsequently, the PCA axis 1 showed an eigenvalue of 0.1974  
206 and the axis 2 an eigenvalue of 0.0659. The first axis explained 19.7% and the second 6.6% of the  
207 total variance. The first four axes explained 36.1% of the variance in total. In the ordination (Fig. 4),  
208 the samples along the primary PCA axis were arranged according to the site-specific mean July air  
209 temperatures, with Polish sites (warm) having negative scores and Finnish sites (cold) positive  
210 scores (Fig. 4a). The warm and cold indicator taxa identified with the PCA ordination (Fig. 4b)  
211 were the same as indicated with the WA optima and GLMs (Fig. 3). The PCA axis 1 scores of the  
212 samples were strongly correlated with the site-specific temperatures having an  $R$  of 0.91,  $R^2$  of 0.82  
213 and  $p < 0.001$ . The RDA results showed that temperature was the most important variable in  
214 explaining chironomid distribution of the examined variables. Of variation explained by the  
215 examined variables (15.4%), temperature explained 78.8%, pH 13.7% and depth 7.5% (Table 2).  
216 Consequently, temperature had clearly the highest  $\lambda_1:\lambda_2$  ratio (1.061) that justified the construction  
217 of the chironomid-based temperature model.

218 Compared to other model types, WA-PLS had the best performance statistics with  
219 respect to its  $R^2_{\text{Jack}}$  and RMSEP (Table 3). The developed WA-PLS model for mean July air  
220 temperature had an  $R^2_{\text{Jack}}$  of 0.88, RMSEP of 0.88 °C and mean and maximum biases of -0.02 and  
221 0.79 °C, respectively (Table 4). Addition of the second regression calibration component reduced  
222 the RMSEP by 8.8% (randomization  $t$ -test significance 0.004). The 1:1 relationship between the  
223 inferred and observed temperatures in the model illustrated that the combined calibration set has a

224 well-structured continuum in its temperature range with relatively even distribution of samples (Fig.  
225 5a).

226 The test of the developed model on the clastic-biogenic varve record from Lake Nurmijärvi  
227 showed similar trends between the chironomid-inferred and meteorologically observed  
228 temperatures over the instrumental period. In both inferred and observed records (Fig. 6a), the  
229 temperatures remained low during the 19<sup>th</sup> century with increased temperatures at the 1930s.  
230 Following intermediate summer temperatures, the climate began to warm in the 1990s and record  
231 highest temperatures synchronously occurred during the 21<sup>th</sup> century. The correlation between the  
232 observed and inferred temperatures at the test site was statistically significant ( $R = 0.72$ ,  $R^2 = 0.52$ ,  
233  $R_{\text{corrected}} = 0.51$ ,  $p < 0.001$ ), although in several samples the temperature difference was larger than  
234 the sample-specific error estimate (Fig. 6b).

235 In the long-core reconstruction, samples 1608-1181 cm (older than 15,000 cal yr BP) had  
236 poor modern analogues according to the MAT suggesting that the early part of the sequence may  
237 not be reliably reconstructed. Nonetheless, the reconstructed values correlated with the primary  
238 PCA axis scores ( $R=0.50$ ,  $p<0.001$ ) indicating that chironomids do respond to the reconstructed  
239 variable in the sediment profile. The chironomid-inferred temperature trends using the East  
240 European model were rather similar to those reconstructed using the Norwegian, Russian and Swiss  
241 models (Fig. 7). However, the new model reconstructed higher temperatures for the initial part of  
242 the sediment record (1600-1500 cm, no age estimate), where poor modern analogues occurred. In  
243 all, the East European model was most similar with the reconstruction derived using the Russian  
244 model, whereas larger differences existed when compared with the results using the Norwegian and  
245 Swiss models. In addition to the early part of the record, the East European model reconstructed  
246 high temperatures between 16,000-12,000 cal yr BP and during the past ~1000 yr. Based on the  
247 new model, the most distinct cold events occurred between 1400-1300 cm (ending at ~17,000-  
248 16,000 cal yr BP) and 2000-1000 cal yr BP. However, the latter cold event occurs in samples with

249 low chironomid count sums and presence of semiterrestrial taxa (see Płóciennik et al. 2011 for  
250 details). When compared with the GISP2 record, the warm period at 15,000 cal yr BP and the  
251 following cooling is well represented. The rapid temperature rise during the early Holocene  
252 suggested by the GISP data and the late Holocene cooling trend in the current record suggest  
253 differences between the regional and global records.

254

## 255 **4. DISCUSSION**

256

### 257 **4. 1. Training set**

258

259           Combination of the Finnish and Polish chironomid datasets yielded a training set with a  
260 temperature gradient of 8.8 °C (11.3-20.1 °C) enabling wider usability with respect to paleoclimate  
261 reconstructions. The cold indicators (Figs 2, 3, 4b) in the combined dataset, such as  
262 *Heterotrissocladius maeaeri*-type, *H. grimshawi*-type, *Psectrocladius calcaratus*-type, *Sergentia*  
263 *coracina*-type, *Micropsectra insignilobus*-type and *Tanytarsus lugens*-type are commonly found  
264 also in the cold lakes of other training sets from Eurasia (Heiri et al. 2011, Self et al. 2011).  
265 Similarly, the warm preferring chironomids, such as *Polypedilum sordens*-type, *Glyptotendipes*  
266 *barbipes*-type, *G. pallens*-type and *Endochironomus albipennis*-type are typical warm indicators in  
267 various other datasets (Heiri et al. 2003, Self et al. 2011). These warm taxa also appear to be more  
268 common in meso-eutrophic lakes, whereas the cold taxa are more often found in oligotrophic sites  
269 (Brooks et al. 2001, Brodersen & Quinlan 2006, Luoto 2011). This occurrence pattern has been  
270 previously documented (Eggermont & Heiri 2012) and is for large part related to the fact that warm  
271 lakes are often more productive and human influenced compared to the naturally oligotrophic cold  
272 lakes. In addition, the results showed that *Paratanytarsus penicillatus*-type, *Dicrotendipes*,  
273 *Procladius* and *Chironomus anthracinus*-type are eurythermic taxa having large temperature

274 tolerances (Figs 3, 4b) that has also been described in various other datasets (Larocque et al. 2006,  
275 Fortin et al. 2015, Nazarova et al. 2015). These taxa aggregate several species that is probably one  
276 of the reasons for their broad tolerance values. Of the most common taxa (Figs 2, 3), only  
277 *Dicrotendipes* did not have a statistically significant relationship with temperature and *P.*  
278 *penicillatus*-type was the only one having a bimodal distribution. These factors inevitably influence  
279 their use as temperature indicators. Although the general temperature indication of the taxa is in  
280 most part similar to the other training sets, there are significant differences in the values of the taxa-  
281 specific temperature optima that are related to the temperature gradients of the respective datasets.  
282 These regional differences in optima will become significant when selecting the training set to be  
283 used in a downcore, seriously affecting the reconstructed quantitative values (Engels et al. 2014,  
284 Fortin et al. 2015).

285         The PCA indicated a humped distribution of the samples in the ordination space (Fig. 4).  
286 The samples were clearly distributed along the primary PCA axis according to their site-specific  
287 temperatures that was also verified by the high correlation ( $R = 0.91$ ,  $R^2 = 0.82$ ,  $p < 0.001$ ) between  
288 the PCA 1 scores and observed temperatures at the sites. Although the ordination plot illustrates that  
289 the secondary gradient also has influence on the assemblages, the PCA axis 2 explained only 6.6%  
290 of the total variance. In addition, the RDA results (Table 2) clearly indicated that temperature is the  
291 most significant variable explaining chironomid distribution among the mutually measured  
292 variables in the Finnish and Polish datasets. Importantly, water depth, which has been found  
293 significant in explaining intralake chironomid distributions in Finland (Luoto 2010) and elsewhere  
294 (Kurek & Cwynar 2009, Engels et al. 2012, Luoto 2012a, 2012b), explained only a minor share of  
295 the chironomid community compositions. Therefore, these results demonstrate that the chironomid  
296 assemblages closely respond to mean July air temperature in the combined dataset, and  
297 consequently justify the development of the East European chironomid-based temperature model.  
298 The primary response of chironomids to temperature has been clearly evidenced in a bulk of

299 distributional studies (Larocque & Hall 2003, Nyman et al. 2005, Brooks et al. 2012) and their  
300 biological response to temperature is also evident (Rossaro 1991, Eggermont & Heiri 2012).  
301 Nonetheless, detecting the potential influence of secondary environmental gradients, such as water  
302 depth, nutrients and DOC, on chironomid-based paleotemperature reconstructions remains  
303 important, especially since their significance may vary in time (Nyman et al. 2008, Shala et al.  
304 2014, Medeiros et al. 2015).

305

## 306 **4.2. Calibration model**

307

308 The developed temperature calibration model used WA-PLS technique, which  
309 outperformed the other tested model types (Table 3). Typical for chironomid-temperature  
310 calibration models (Heiri et al. 2011), the use of two WA-PLS components was statistically  
311 justified. The model's statistical performance (Fig. 5), measured in  $R^2_{\text{Jack}}$ , was comparable with  
312 other chironomid-based temperature models (Heiri et al. 2011, Holmes et al. 2011) but in its  
313 RMSEP (0.88 °C, 10% of calibration set gradient) it outperformed several of the other models,  
314 many of them having RMSEPs  $>1$  °C (Barley et al. 2006, Porinchu et al. 2009, Nazarova et al.  
315 2011). Compared to the new East European model, the original latitudinal Finnish temperature  
316 model had lower  $R^2_{\text{Jack}}$  (0.78) but also lower RMSEP (0.72 °C, 12.4% of calibration set gradient)  
317 (Table 4). However, since RMSEP is inherently influenced by the gradient length of the examined  
318 variable, it may be more useful to compare the RMSEPs in relation to the temperature gradients. In  
319 this sense, the RMSEP is more favorable in the combined model.

320 The combination of the Finnish and Polish datasets resulted as a consistent continuum in  
321 the model's predictive abilities, as the Polish sites increased the temperature gradient of the model  
322 towards warmer temperatures (Fig. 5a). Longer environmental gradients will help in situations  
323 where past climate conditions approach the specific dataset's temperature limits (Birks et al. 2003).

324 Slight distortions at both ends of the temperature gradient were observed (Fig. 5b) that is inherent in  
325 WA-PLS models (Heiri & Lotter 2010). This distortion, i.e. edge-effect, causes underestimation of  
326 warm temperatures and overestimation of cold temperatures, and hence potentially smoothen  
327 reconstructions.

328

### 329 **4.3. Reconstructions**

330

331 The best means to verify environmental reconstructions is to compare them with instrumentally  
332 measured data (Larocque et al. 2009, Larocque-Tobler et al. 2015). Our test site, Lake Nurmijärvi  
333 with sediments constituting of clastic biogenic varves, is located in southcentral Finland, close to  
334 the warm end of the temperature gradient of the original Finnish training set (Fig. 1). The  
335 reconstruction results showed that the East European model has the ability to accurately predict  
336 downcore temperatures, as it well-depicted the cold temperatures of the 19<sup>th</sup> century, the increased  
337 temperatures of the 1930s and the rapid warming that began in the 1980s (Fig. 6). The mean  
338 difference in the inferred values compared to the observed was only 0.3 °C but the largest  
339 overestimation was 3.0 °C and underestimation 2.7 °C. The biased values are most likely related to  
340 lags in chironomid response times, since many taxa have long life cycles and their dispersal,  
341 although fast compared to many other biological proxies (Wu et al. 2015), can take up to seven  
342 years (Pinder 1986). The correlation between reconstructed and observed temperatures was higher  
343 than in the previous study where the latitudinal Finnish model was used (Luoto & Ojala 2017),  
344 clearly suggesting that the new model has better prediction accuracy and reliability compared to the  
345 original model.

346         Since the model had solid performance statistics and it was able to reconstruct similar  
347 temperatures with the observational record in southern Finland, we also applied it to a long-core  
348 taken from the Żabieniec paleolake in Poland. Importantly, the chironomid-inferred values showed

349 significant correlation with the primary ordination axis scores verifying that chironomids respond to  
350 temperature in the Żabieniec record. The previous study from the site demonstrated that  
351 chironomid-based temperature models from outside the geographical area reconstructed partly  
352 differing temperatures (Płóciennik et al. 2011). The present results showed that the developed East  
353 European model reconstructed temperatures that mostly resemble those reconstructed using the  
354 Russian model (Self et al. 2011) (Fig. 7), whereas distinct differences were apparent when  
355 compared with the Swiss (Heiri & Lotter 2005) and Norwegian models (Brooks & Birks 2001)  
356 (Fig. 7). These differences include very low temperatures in the initial part of the record and the  
357 absence of the late Holocene cooling trend (Wanner et al. 2015). The early phase of the record may  
358 be connected with the warm Kamion phase previously described from Poland (Manikowska 1995),  
359 however, this remains uncertain due to lack of detailed chronological control in the bottom part of  
360 the Żabieniec sediment sequence. Although the present interpretations are based solely on mean  
361 July air temperature and there is no data on winter conditions or vegetational season length, it may  
362 still be speculated that the climate conditions during the early phase of the record were glacial, but  
363 because of high continentality summers were warm as in Siberia (Klimanov 1997). This  
364 interpretation would be logical also considering that the East European and Russian models produce  
365 similar warm temperatures for this phase differing from those derived using the Swiss and  
366 Norwegian models (Fig. 6).

367           It is possible that the late Glacial temperatures could have been colder in Żabieniec than  
368 the lowest temperatures represented by the calibration sites. However, the reconstructed  
369 temperatures are not close the limits of the model (11 °C) but remain at >14 °C (Fig. 7). If the  
370 actual temperatures would have been colder and the chironomid taxa would have consisted solely of  
371 taxa with coldest temperature preferences, the WA-PLS model would have the potential to  
372 extrapolate beyond the cold gradient end (Velle et al. 2011). This was not the case in the present  
373 data, where late Glacial sequences consisted of taxa with intermediate temperature optima, such as

374 *Procladius* and *Tanytarsus pallidicornis*-type (Fig. 7). These taxa are also known to have wider  
375 trophic tolerances (Brodersen & Quinlan 2006), which could reflect elevated nutrient condition  
376 during the early part of the sediment profile. In contrast, the Norwegian, Russian and Swiss  
377 calibration models all reconstruct consistently colder late Glacial temperatures than the East  
378 European model. This is probably related to the compared calibration models having generally  
379 colder lakes among the training set sites, and hence, the new model would benefit from inclusion on  
380 even colder sites than it currently has. Despite the extrapolation capabilities of the WA-PLS  
381 method, it is clear that the East European model can be reliable only within its temperature gradient  
382 (11-20 °C), with decreasing reliability towards the gradient ends. Consequently, the coldest and  
383 warmest episodes in long sediment records, such as the Żabieniec record, should be considered  
384 cautiously when observing the reconstructed values, although at the same time the trends may be  
385 realistic. It is also noteworthy that the late Glacial chironomid assemblages had poor modern  
386 analogues in the calibration set that decreases the reliability of the new reconstruction during this  
387 early phase of the record.

388         Similar to the other chironomid-based reconstructions, the new reconstruction did not  
389 depict significant temperature drop during the cold Younger Dryas period. There are also no distinct  
390 changes in the taxonomic composition at this time (Płóciennik et al. 2011, Fig. 7) that could  
391 indicate other driving factors that would potentially reduce the temperature signal. This period was  
392 unusually cold in Scandinavia (Brooks & Birks 2000, Wohlfarth et al. 2018) but in several studies  
393 from Poland (Zawiska et al. 2015, Pawłowski et al. 2015, 2016a, 2016b) and Central Europe  
394 (Larocque-Tobler et al. 2010), the summer temperature drop during the Younger Dryas has been  
395 relatively muted compared to the British Isles, the Baltic region and the northern parts of the  
396 continent (Heiri et al. 2014). Therefore, the present results are consistent with the previous studies  
397 from Poland showing intra-European differences. Compared to the other chironomid-based  
398 reconstructions from Żabieniec, the East European model reconstructs similar 16-17 °C



399 temperatures, with the exception of the Norwegian model, which indicates slightly lower  
400 temperatures (Fig. 7).

401           Compared to hemispheric temperatures reflected by the GISP2 ice core record (Cuffey &  
402 Clow 1997; Alley 2000), the current reconstruction does not suggest similar increase in early  
403 Holocene temperatures (Fig. 7). The rapid early Holocene temperature increase has been described  
404 from several lake sediment records from northern Europe (Brooks & Birks 2000, Engels et al. 2014,  
405 Luoto et al. 2014, Shala et al. 2017, Helmens et al. 2018) and the European Alps (Samartin et al.  
406 2012). The increase in *Lauterborniella* between 10,000 and 8000 cal yr BP can be related to  
407 nutrient conditions, since in addition to high temperature optimum, it is known to thrive in more  
408 nutrient-enriched lakes (Brooks et al. 2007). However, the warming associated with the increase in  
409 *Lauterborniella* is consistent with the increased temperatures in the GISP2 record following the  
410 cold early Holocene. The late Holocene cooling trend is not apparent in the GISP2 record, although  
411 clearly seen from the present results and several other records from Poland (Zawiska et al. 2015,  
412 Pawłowski et al. 2015, 2016b) suggesting regional deviation from hemispheric temperatures.  
413 Nonetheless, it should be noted that the temperature decrease reconstructed from Żabieniec between  
414 2000 and 1000 cal yr BP is not reliable owing to dominance of semiterrestrial chironomid taxa and  
415 low count sums (Płóciennik et al. 2011). Compared to the reconstructions performed using the other  
416 chironomid-based models and the GISP2 record, the temperatures reconstructed using the East  
417 European model showed a distinct warming during the past 1000 yr, with a short-lived drop in  
418 temperatures during the Little Ice Age. In general, the reconstruction of the Holocene temperatures  
419 in Żabieniec paleolake closely resembles those from elsewhere in Europe (Davis et al. 2003, Luoto  
420 et al. 2010, Engels et al. 2014) combined with distinct local features (Zawiska et al. 2015,  
421 Pawłowski et al. 2015, 2016b), hence signifying the reliability of the reconstruction.

422

## 423 **5. CONCLUSIONS**

424

425 Merging the Finnish and Polish chironomid-based training sets resulted as a valid  
426 calibration model for mean July air temperature with an extended temperature gradient and  
427 improved applicability. The temperature indicators were similar to what has been found in previous  
428 studies, however, the numerical optima more accurately adjusted for the study area. The statistical  
429 tests showed that chironomids were responding most strongly to temperature, hence enabling  
430 construction of the enhanced model. Compared to previous chironomid-temperature models in  
431 general, the new East European model has solid performance statistics.

432 The model validation in a Finnish annually laminated lake sediment record, covering the  
433 observational temperature period beginning from the 1830s, showed that the model better predicts  
434 paleotemperatures compared to the original Finnish model. Since the inferred temperatures  
435 correlated strongly with the instrumental record, the model can be considered solid with respect to  
436 its predictive abilities and applicability in downcore profiles from Eastern Europe. The  
437 reconstructed temperatures using the East European model in the long-core from the Polish  
438 paleolake Żabieniec, covering the past ~20,000 yr, were more similar to temperatures reconstructed  
439 using the Russian chironomid-based model than the ones reconstructed using the Swiss and  
440 Norwegian models. The reconstructed temperature trends were comparable to previous studies from  
441 Poland but significantly different from hemispheric paleotemperature estimates signifying the  
442 importance of local reconstructions in understanding past climate oscillations.

443 Although the model is designed for Finnish and Polish sites as a preset, it can be useful in  
444 other areas of Eastern Europe as well. In the future, the East European model can be further  
445 developed especially by including additional calibration sites from the Baltic Countries that would  
446 promote stability of the model. In all, the present results demonstrate the usability and sensitivity of  
447 fossil chironomids as quantitative paleoclimate indicators.

448

449 *Acknowledgements.* This study was funded by the Emil Aaltonen Foundation (grants 160156,  
450 170161 and 180151), grant of Polish Ministry of Science and Higher Education (2 P04E 02228),  
451 SYNTHESYS EU grant for Żabieniec chironomid sequence studies, Polish Geological Institute –  
452 National Research Institute grants (61.3608.1401.00.0 and 65-3608-1401-00-0) and SYNTHESYS  
453 European Community Research Infrastructure Action under the FP7 "Capacities" Program" for  
454 Polish Chironomidae calibration set. Support for mobility by the EU Climate-KIC's Pioneers into  
455 Practice programme is deeply appreciated. We are grateful for the three journal reviewers for their  
456 constructive comments and help to improve the manuscript.

457

#### 458 LITERATURE CITED

459

460 Alley RB (2000) The Younger Dryas cold interval as viewed from central Greenland. *Quat Sci Rev*  
461 19:213–226

462

463 Barley EM, Walker IR, Kurek J, Cwynar LC, Mathewes RW, Gajewski K, Finney BP (2006) A  
464 northwest North American training set: distribution of freshwater midges in relation to air  
465 temperature and lake depth. *J Paleolimnol* 36:295–314

466

467 Bigler C, Heiri O, Krskova R, Lotter AF, Sturm M (2006) Distribution of diatoms, chironomids and  
468 cladocerans in surface sediments of thirty mountain lakes in southeastern Switzerland. *Aquat Sci*  
469 68:154–171

470

471 Birks HJB, Mackay A, Battarbee RW, Birks J, Oldfield F (2003) Quantitative palaeoenvironmental  
472 reconstructions from Holocene biological data. *Global change in the Holocene* pp. 107–123

473

474 Brodersen KP, Quinlan R (2006) Midges as palaeoindicators of lake productivity, eutrophication  
475 and hypolimnetic oxygen. *Quat Sci Rev* 25:1995–2012  
476

477 Brooks SJ (2006) Fossil midges (Diptera: Chironomidae) as palaeoclimatic indicators for the  
478 Eurasian region. *Quat Sci Rev* 25:1894–1910  
479

480 Brooks SJ, Birks HJB (2001) Chironomid-inferred air temperatures from Lateglacial and Holocene  
481 sites in north-west Europe: progress and problems. *Quat Sci Rev* 20:1723–1741  
482

483 Brooks SJ, Axford Y, Heiri O, Langdon PG, Larocque-Tobler I (2012) Chironomids can be reliable  
484 proxies for Holocene temperatures. A comment on Velle et al. (2010). *Holocene* 22:1495–1500  
485

486 Brooks SJ, Langdon PG, Heiri O (2007) The identification and use of Palaeartic Chironomidae  
487 larvae in palaeoecology. QRA Technical Guide No. 10. Quaternary Research Association, London.,  
488 276 pp  
489

490 Brooks SJ, Bennion H, Birks HJB (2001) Tracing lake trophic history with a chironomid–total  
491 phosphorus inference model. *Freshw Biol* 46:513–533  
492

493 Cuffey KM, Clow GD (1997) Temperature, accumulation, and ice sheet elevation in central  
494 Greenland through the last deglacial transition. *J Geophys Res* 102:26383–26396  
495

496 Davis BA, Brewer S, Stevenson AC, Guiot J (2003) The temperature of Europe during the  
497 Holocene reconstructed from pollen data. *Quat Sci Rev* 22:1701–1716  
498

499 Eggermont H, Heiri O (2012) The chironomid-temperature relationship: expression in nature and  
500 palaeoenvironmental implications. *Biol Rev* 87:430–456  
501

502 Engels S, Self AE, Luoto TP, Brooks SJ, Helmens KF (2014) A comparison of three Eurasian  
503 chironomid-climate calibration datasets on a W-E continentality gradient and the implications for  
504 quantitative temperature reconstructions. *J Paleolimnol* 51:529–547  
505

506 Engels S, Cwynar LC, Rees AB, Shuman BN (2012) Chironomid-based water depth  
507 reconstructions: an independent evaluation of site-specific and local inference models. *J*  
508 *Paleolimnol* 48:693–709  
509

510 Fortin MC, Medeiros AS, Gajewski K, Barley EM, Larocque-Tobler I, Porinchu DF, Wilson SE  
511 (2015) Chironomid-environment relations in northern North America. *J Paleolimnol* 54:223–237  
512

513 Hammer Ø, Harper DAT, Ryan PD (2001) PAST: Paleontological statistics software package for  
514 education and data analysis. *Palaeontol Electron* 4:1–9  
515

516 Heiri O, Lotter AF (2010) How does taxonomic resolution affect chironomid-based temperature  
517 reconstruction? *J Paleolimnol* 44:589–601  
518

519 Heiri O, Lotter AF (2005) Holocene and Late Glacial summer temperature in the Swiss Alps based  
520 on fossil assemblages of aquatic organisms: a review. *Boreas* 34:506–516  
521

522 Heiri O, Brooks SJ, Birks HJB, Lotter AF (2011) A 274-lake calibration data-set and inference  
523 model for chironomid-based summer air temperature reconstruction in Europe. *Quat Sci Rev*  
524 30:3445–3456  
525

526 Heiri O, Lotter AF, Hausmann S, Kienast F (2003) A chironomid-based Holocene summer air  
527 temperature reconstruction from the Swiss Alps. *Holocene* 13:477–484  
528

529 Heiri O et al. (2014) Validation of climate model-inferred regional temperature change for late-  
530 glacial Europe. *Nat Com* 5:4914  
531

532 Helmens KF, Katrantsiotis C, Salonen JS, Shala S, Bos JAA, Engels S, Kuosmanen N, Luoto TP,  
533 Väiliranta M, Luoto M, Ojala AEK, Risberg J, Weckström J (2018) Warm summers and rich biotic  
534 communities during N-Hemisphere deglaciation. *Global Planet Change* 167:61–73  
535

536 Holmes N, Langdon PG, Caseldine C, Brooks SJ, Birks HJB (2011) Merging chironomid training  
537 sets: implications for palaeoclimate reconstructions. *Quat Sci Rev* 30:2793–2804  
538

539 Ilyashuk EA, Koinig KA, Heiri O, Ilyashuk BP, Psenner R (2011) Holocene temperature variations  
540 at a high-altitude site in the Eastern Alps: a chironomid record from Schwarzsee ob Sölden, Austria.  
541 *Quat Sci Rev* 30:176–191  
542

543 Juggins S (2007) C2: Software for ecological and palaeoecological data analysis and visualisation  
544 (user guide version 1.5). Newcastle upon Tyne, Newcastle University  
545

546 Klimanov VA (1997) Late glacial climate in northern Eurasia: the last climatic cycle. *Quat Int*  
547 41:141–152  
548

549 Kurek J, Cwynar LC (2009) Effects of within-lake gradients on the distribution of fossil  
550 chironomids from maar lakes in western Alaska: implications for environmental reconstructions.  
551 *Hydrobiologia* 62:337–52  
552

553 Lamentowicz M., Balwierz Z, Forysiak J, Płóciennik M, Kittel P, Kloss M, Twardy J, Żurek S,  
554 Pawlyta J (2009) Multiproxy study of anthropogenic and climatic changes in the last two millennia  
555 from a small mire in central Poland. *Hydrobiologia* 631:213–230  
556

557 Larocque I, Hall RI (2003) Chironomids as quantitative indicators of mean July air temperature:  
558 validation by comparison with century-long meteorological records from northern Sweden. *J*  
559 *Paleolimnol* 29:475–493  
560

561 Larocque I, Pienitz R, Rolland N (2006) Factors influencing the distribution of chironomids in lakes  
562 distributed along a latitudinal gradient in northwestern Quebec, Canada. *Can J Fish Aquat Sci*  
563 63:1286–1297  
564

565 Larocque-Tobler I, Filipiak J, Tylmann W, Bonk A, Grosjean M (2015) Comparison between  
566 chironomid-inferred mean-August temperature from varved Lake Żabińskie (Poland) and  
567 instrumental data since 1896 AD. *Quat Sci Rev* 111:35–50  
568

569 Larocque I, Grosjean M, Heiri O, Bigler C, Blass A (2009) Comparison between chironomid-  
570 inferred July temperatures and meteorological data AD 1850–2001 from varved Lake Silvaplana,  
571 Switzerland. *J Paleolimnol* 41:329–342  
572

573 Larocque-Tobler I, Heiri O, Wehrli M (2010) Late Glacial and Holocene temperature changes at  
574 Egelsee, Switzerland, reconstructed using subfossil chironomids. *J Paleolimnol* 43:649–666  
575

576 Linderholm HW et al. (2018) Arctic hydroclimate variability during the last 2000 years – current  
577 understanding and research challenges. *Clim Past* 14:1–42  
578

579 Luoto TP (2012a) Intra-lake patterns of aquatic insect and mite remains. *J Paleolimnol* 47:141–157  
580

581 Luoto TP (2012b) Spatial uniformity in depth optima of midges: evidence from sedimentary  
582 archives of shallow Alpine and boreal lakes. *J Limnol* 71:228–232  
583

584 Luoto TP (2011) The relationship between water quality and chironomid distribution in Finland – A  
585 new assemblage-based tool for assessments of long-term nutrient dynamics. *Ecol Indic* 11:255–262  
586

587 Luoto TP (2010) Hydrological change in lakes inferred from midge assemblages through use of an  
588 intralake calibration set. *Ecol Monogr* 80:303–329  
589

590 Luoto TP (2009) Subfossil Chironomidae (Insecta: Diptera) along a latitudinal gradient in Finland:  
591 development of a new temperature inference model. *J Quat Sci* 24:150–158  
592



593 Luoto TP, Ojala AEK (2017) Meteorological validation of chironomids as a paleotemperature  
594 proxy using varved lake sediments. *Holocene* 27:870–878  
595

596 Luoto TP, Ojala AEK, Arppe L, Brooks SJ, Kurki E, Oksman M, Wooller MJ, Zajączkowski M  
597 (2018) Synchronized proxy-based temperature reconstructions reveal mid- to late Holocene climate  
598 oscillations in High Arctic Svalbard. *J Quat Sci* 33:93–99  
599

600 Luoto TP, Rantala MV, Galkin A, Rautio M, Nevalainen L (2016) Environmental determinants of  
601 chironomid communities in remote northern lakes across the treeline – Implications for climate  
602 change assessments. *Ecol Indic* 61:991–999  
603

604 Luoto TP, Kaukolehto M, Weckström J, Korhola A, Väliranta M (2014) New evidence of warm  
605 early-Holocene summers in subarctic Finland based on an enhanced regional chironomid-based  
606 temperature calibration model. *Quat Res* 81:50–62  
607

608 Luoto TP, Kultti S, Nevalainen L, Sarmaja-Korjonen K (2010) Temperature and effective moisture  
609 variability in southern Finland during the Holocene quantified with midge-based calibration models.  
610 *J Quat Sci* 25:1317–1326  
611

612 Manikowska B (1995) Aeolian activity differentiation in the area of Poland during the period 20-8  
613 ka BP. *Biuletyn Peryglacjalny* 34:127–165  
614

615 McCarroll D (2015) ‘Study the past, if you would divine the future’: a retrospective on measuring  
616 and understanding Quaternary climate change. *J Quat Sci* 30:154–187  
617

618 Medeiros AS, Gajewski K, Porinchu DF, Vermaire JC, Wolfe BB (2015) Detecting the influence of  
619 secondary environmental gradients on chironomid-inferred paleotemperature reconstructions in  
620 northern North America. *Quat Sci Rev* 124:265–274  
621

622 Nazarova L, Self AE, Brooks SJ, van Hardenbroek M, Herzsuh U, Diekmann B (2015) Northern  
623 Russian chironomid-based modern summer temperature data set and inference models. *Global*  
624 *Planet Change* 134:10–25  
625

626 Nazarova L, Herzsuh U, Wetterich S, Kumke T, Pestryakova L (2011) Chironomid-based  
627 inference models for estimating mean July air temperature and water depth from lakes in Yakutia,  
628 northeastern Russia. *J Paleolimnol* 45:57–71  
629

630 Nyman M, Weckström J, Korhola A (2008) Chironomid response to environmental drivers during  
631 the Holocene in a shallow treeline lake in northwestern Fennoscandia. *Holocene* 18:215–227  
632

633 Nyman M, Korhola A, Brooks SJ (2005) The distribution and diversity of Chironomidae (Insecta:  
634 Diptera) in western Finnish Lapland, with special emphasis on shallow lakes. *Global Ecol Biogeogr*  
635 14:137–153  
636

637 Ojala AEK, Mattila J, Virtasalo J, Kuva J, Luoto TP (2018) Seismic deformation of varved  
638 sediments in southern Fennoscandia at 7400 cal BP. *Tectonophysics* 744:58-71  
639

640 Ojala AEK, Luoto TP, Virtasalo JJ (2017) Establishing a high-resolution surface sediment  
641 chronology with multiple dating methods – Testing <sup>137</sup>Cs determination with Nurmijärvi clastic-  
642 biogenic varves. *Quat Geochronol* 37:32–41

643

644 Pawłowski D, Borówka RK, Kowalewski G, Luoto TP, Milecka K, Nevalainen L, Okupny D,  
645 Płóciennik M, Woszczyk M, Tomkowiak J, Zieliński T (2016a) The response of flood-plain  
646 ecosystems to the Late Glacial and Early Holocene hydrological changes: A case study from a small  
647 Central European river valley. *Catena* 147:411–428

648

649 Pawłowski D, Borówka RK, Kowalewski G, Luoto TP, Milecka K, Nevalainen L, Okupny D,  
650 Zieliński T, Tomkowiak J (2016b) Late Weichselian and Holocene record of the  
651 paleoenvironmental changes in a small river valley in Central Poland. *Quat Sci Rev* 135:24–40

652

653 Pawłowski D, Płóciennik M, Brooks SJ, Luoto TP, Milecka K, Nevalainen L, Peyron O, Self A,  
654 Zieliński T (2015) A multiproxy study of Younger Dryas and Early Holocene climatic conditions  
655 from the Grabia River palaeo-oxbow lake (central Poland). *Palaeogeogr Palaeoclimatol Palaeoecol*  
656 438:34–50

657

658 Paasivirta L (2014) Checklist of the family Chironomidae (Diptera) of Finland. *ZooKeys* 441:63–90

659

660 Pinder LCV (1986) Biology of freshwater Chironomidae. *Annu Rev Entomol* 31:1–23

661

662 Płóciennik M, Self A, Birks HJB, Brooks SJ (2011) Chironomidae (Insecta: Diptera) succession in  
663 Żabieniec bog and its palaeo-lake (central Poland) through the Late Weichselian and Holocene.  
664 *Palaeogeogr Palaeoclimatol Palaeoecol* 307:150–167

665

666 Porinchi D, Rolland N, Moser K (2009) Development of a chironomid-based air temperature  
667 inference model for the central Canadian Arctic. *J Paleolimnol* 41:349–368

668

669 Rantala MV, Luoto TP, Nevalainen L (2016) Temperature controls organic carbon sequestration in  
670 a subarctic lake. *Sci Rep* 6:34780

671

672 Rossaro B (1991) Chironomids and water temperature. *Aquat Insects* 13:87–98

673

674 Sæther OA, Spies M (2013) Fauna Europaea: Chironomidae. *Fauna Europaea: Diptera Nematocera*.  
675 *Fauna Europaea* version, 2.2

676

677 Samartin S, Heiri O, Vescovi E, Brooks SJ, Tinner W (2012) Lateglacial and early Holocene  
678 summer temperatures in the southern Swiss Alps reconstructed using fossil chironomids. *J Quat Sci*  
679 *27:279–289*

680

681 Self A, Brooks SJ, Birks HJB, Nazarova LB, Porinchu D, Odland A, Yang H, Jones VJ (2011) The  
682 influence of temperature and continentality on modern chironomid assemblages in high-latitude  
683 Eurasian lakes: development and application of new chironomid-based climate-inference models in  
684 northern Russia. *Quat Sci Rev* 30:1122–1141

685

686 Shala S, Helmens KF, Luoto TP, Salonen JS, Väiliranta M, Weckström J (2017) Comparison of  
687 quantitative Holocene temperature reconstructions using multiple proxies from a northern boreal  
688 lake. *Holocene* 27:1745–1755

689

690 Shala S, Helmens KF, Luoto TP, Väiliranta M, Weckström J, Salonen JS, Kuhry P (2014)  
691 Evaluating environmental drivers of Holocene changes in water chemistry and aquatic biota  
692 composition at Lake Loitsana, NE Finland. *J Paleolimnol* 52:311–329

693

694 Šmilauer P, Lepš J (2014) *Multivariate analysis of ecological data using CANOCO 5*. Cambridge  
695 University Press

696

697 Velle G, Kongshavn K, Birks HJB (2011) Minimizing the edge-effect in environmental  
698 reconstructions by trimming the calibration set: Chironomid-inferred temperatures from  
699 Spitsbergen. *Holocene* 21:417–430

700

701 von Gunten L, Heiri O, Bigler C, van Leeuwen J, Casty C, Lotter A., Sturm M (2008) Seasonal  
702 temperatures for the past 400 years reconstructed from diatom and chironomid assemblages in a  
703 high-altitude lake (Lej da la Tscheppa, Switzerland). *J Paleolimnol* 39:283–299

704

705 Wanner H, Mercolli L, Grosjean M, Ritz SP (2015) Holocene climate variability and change; a  
706 data-based review. *J Geol Soc* 172, 254–263

707

708 Wohlfarth B, Luoto TP, Muschitiello F, Väiliranta M, Björk S, Davies S, Kylander M, Ljung K,  
709 Reimer P, Smittenberg RH (2018) Climate and environment in southwest Sweden 15.3 – 11.3 cal.  
710 ka BP. *Boreas* 47:687-710

711

712 Wu D, Zhao X, Liang S, Zhou T, Huang K, Tang B, Zhao W (2015) Time-lag effects of global  
713 vegetation responses to climate change. *Glob Change Biol* 21:3520–3531

714

715 Zawiska I, Słowiński M, Correa-Metrio A, Obremaska M, Luoto TP, Nevalainen L, Woszczyk M,  
716 Milecka K (2015) The response of a shallow lake and its catchment to Late Glacial climate changes  
717 – A case study from eastern Poland. *Catena* 126:1–10

718 **Tables**

719 **Table 1.** Characteristics of the study sites in the Finnish, Polish and the combined East European  
 720 chironomid-based temperature datasets. Mean values are given in brackets.

	Finnish	Polish	Combined
Number of sites (N)	114	98	212
Number of taxa (N)	111	100	142
Latitude (°N)	60.13-69.55 (65.91)	49.19-54.68 (52.60)	49.19-69.55 (59.60)
Longitude (°E)	22.00-30.13 (26.55)	14.51-23.42 (18.42)	14.51-30.13 (22.69)
Elevation (m a.s.l.)	4-405 (157)	4-1624 (196)	4-1624 (174)
Temperature gradient (°C)	11.3-17.1 (14.4)	11.6-20.1 (18.6)	11.3-20.1 (16.4)
Sampling depth (m)	0.5-7.0 (2.3)	0.3-15.0 (8.8)	0.3-15.0 (5.7)
pH	4.6-8.4 (6.5)	5.1-9.8 (8.3)	4.6-9.8 (7.5)

721

722

723

724

725

726

727

728

729

730

731

732

733

734

735

736 Table 2. Redundancy analysis (RDA) results for the combined East European chironomid dataset.

737 All examined variables together explain 15.4% of the total variance.

Variable	$\lambda_1:\lambda_2$	Contribution (%)	<i>F</i>	<i>p</i> ( <i>p</i> <sub>bonferroni adjusted</sub> )
Mean July air temperature	1.061	78.8	26.0	0.001 (0.003)
pH	0.563	13.7	4.6	0.001 (0.003)
Water depth	0.398	2.5	2.5	0.002 (0.006)

738

739

740

741

742

743

744

745

746

747

748

749

750

751

752

753

754

755

756

757 Table 3. Comparison of performance statistics using different model types (WA = weighted  
 758 averaging, PLS = partial least squares) in the development of the East European chironomid-based  
 759 calibration model. The model deemed most suitable for downcore reconstructions is marked with  
 760 boldtype.

Calibration model type	Coefficient of determination ( $R^2_{\text{jack}}$ )	Root mean squared error of prediction (RMSEP, °C)	Maximum bias (°C)	Reduction in RMSEP (%)
WA <sub>inverse deshrinking</sub>	0.86	0.96	1.22	
WA <sub>classical deshrinking</sub>	0.86	1.01	0.76	
PLS <sub>component 1</sub>	0.84	1.04	1.51	
PLS <sub>component2</sub>	0.86	0.96	0.93	7.99
WA-PLS <sub>component1</sub>	0.86	0.97	1.24	
<b>WA-PLS<sub>component2</sub></b>	<b>0.88</b>	<b>0.88</b>	<b>0.79</b>	<b>8.78</b>

761

762

763

764

765

766

767

768

769

770

771

772

773

774



775 Table 4. Performance statistics of the developed East European chironomid-based temperature  
 776 calibration model compared with the original Finnish model (Luoto 2009).

	East European model	Finnish model
Number of sites (N)	212	82
Number of taxa (N)	142	110
Model type	WA-PLS, component 2	WA-PLS, component 2
Coefficient of determination ( $R^2_{\text{jack}}$ )	0.88	0.78
Root mean squared error of prediction (RMSEP)	0.88 °C	0.72 °C
Maximum bias	0.79 °C	0.79 °C

777

778

779

780

781

782

783

784

785

786

787

788

789

790

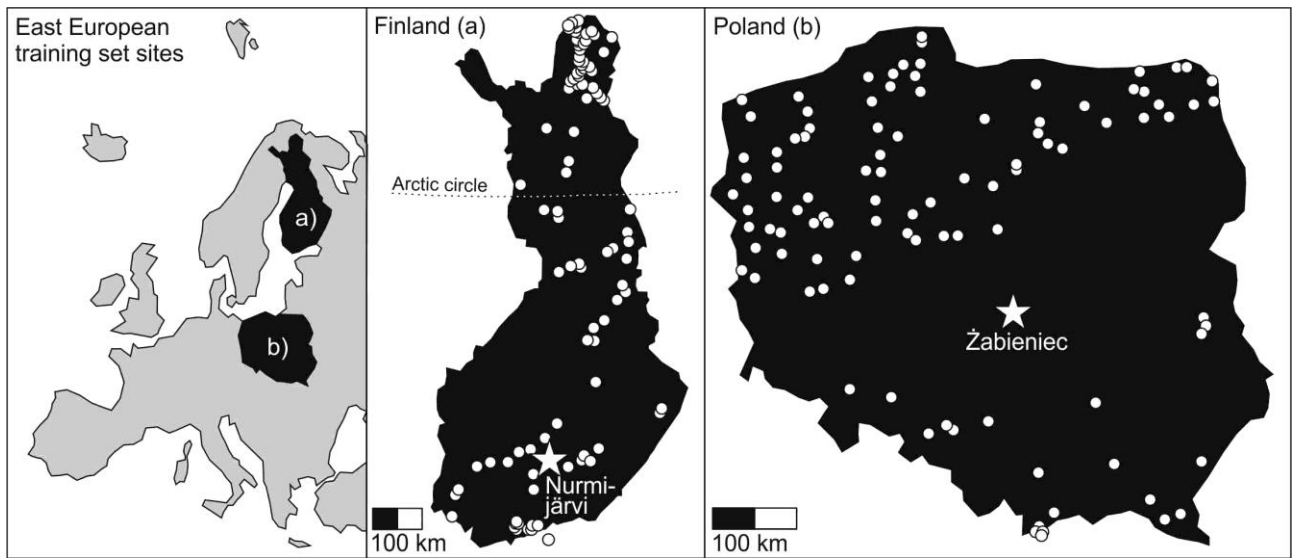
791

792

793

794

795 **FIGURES**



796

797 Fig. 1. Calibration sites of the East European chironomid-based temperature training set. The  
798 Finnish dataset ( $60^{\circ}13' - 69^{\circ}55'N$ ) include 114 (a) and the Polish dataset ( $49^{\circ}19' - 54^{\circ}68'N$ ) 98 lakes  
799 (b). The downcore study site Żabieniec (Poland) and Nurmijärvi (Finland) are marked with stars.

800

801

802

803

804

805

806

807

808

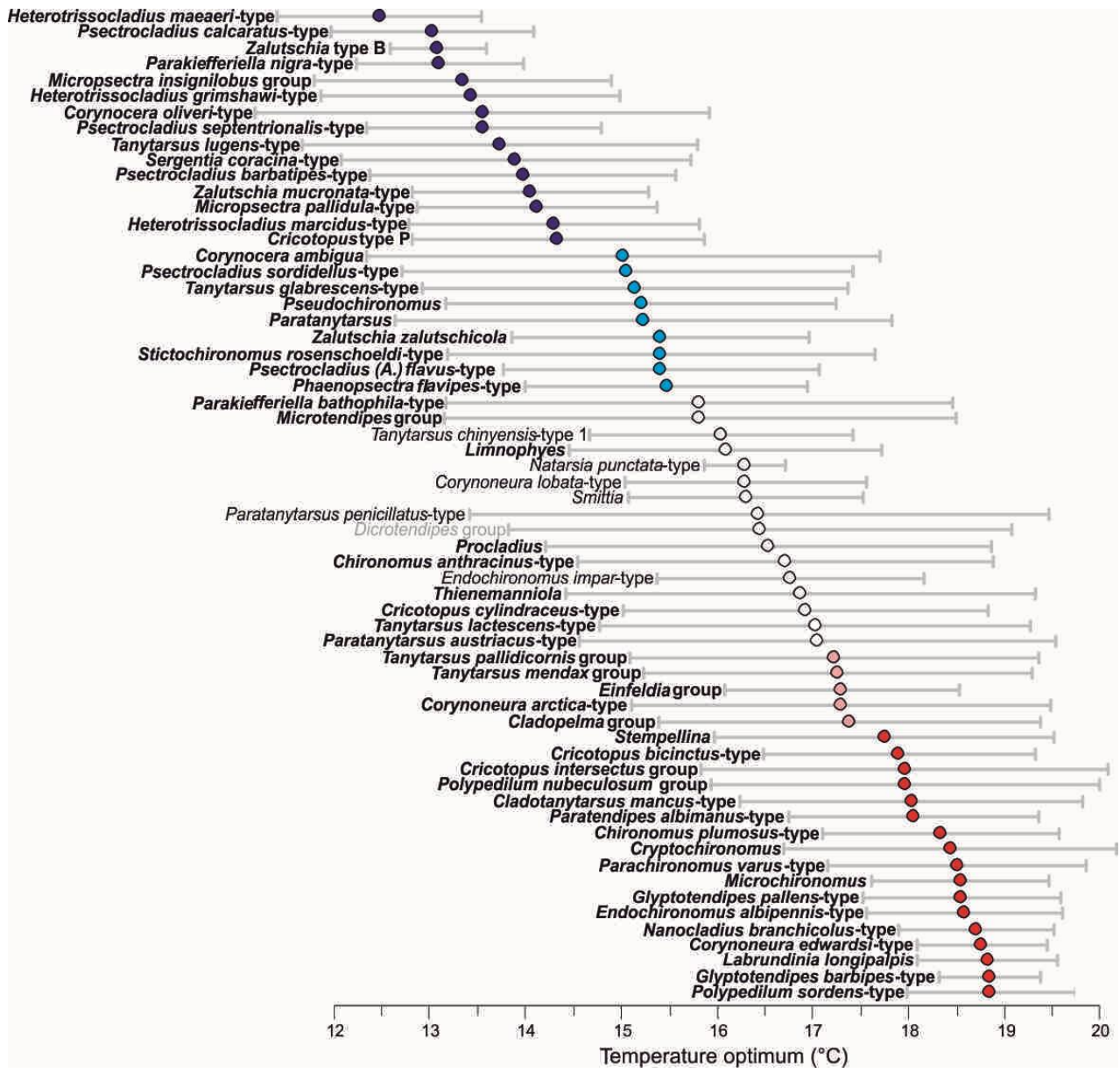
809

810

811

812

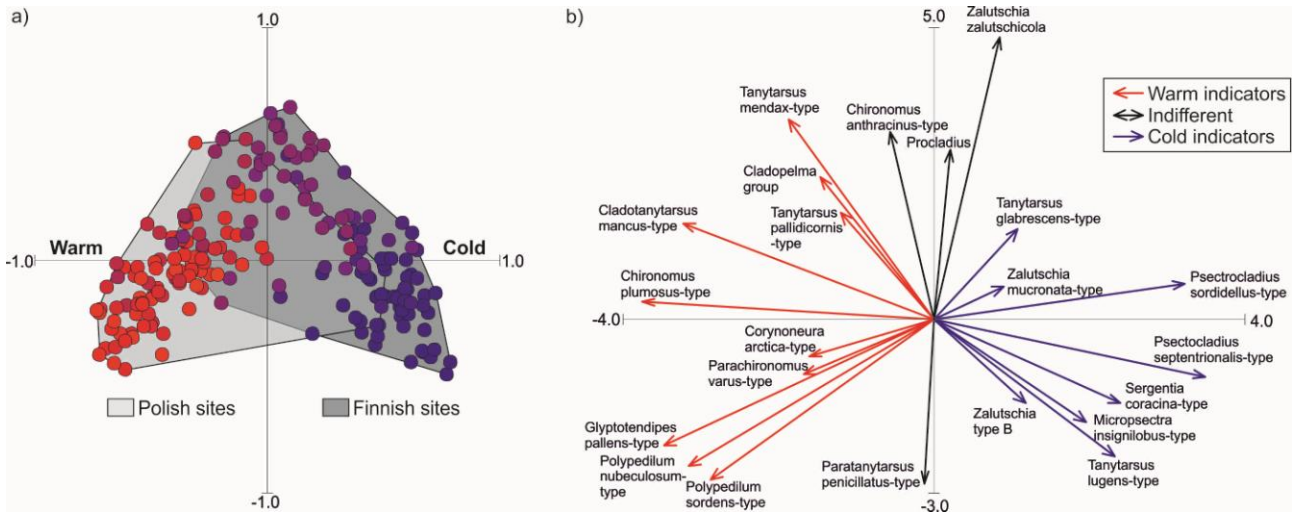




816

817 Fig. 3. Chironomid mean July air temperature optima (weighted averaging) of the most common  
 818 taxa ( $N > 5$ ) in the combined East European dataset. The cold indicators are marked with blue,  
 819 intermediate taxa with white and warm indicators with red. Taxa having statistically significant  
 820 linear relationships with temperature are marked in bold type and nonlinear fit with regular font.  
 821 The only taxon (*Dicrotendipes*) with no significant relationship is marked in grey.

822



823

824 Fig. 4. Principal Component Analysis (PCA) ordination plots for samples (a) and  
 825 based on surface sediment chironomid assemblages from lakes in Poland and Finland. The first  
 826 (horizontal) PCA axis ( $\lambda = 0.20$ ) explains 19.7% and the second (vertical) PCA axis ( $\lambda = 0.07$ ) 6.6%  
 827 of the total variance. The samples (sites) are colored according to their temperature from warm (red)  
 828 to cold (blue) and the envelopes represent the different geographical regions.

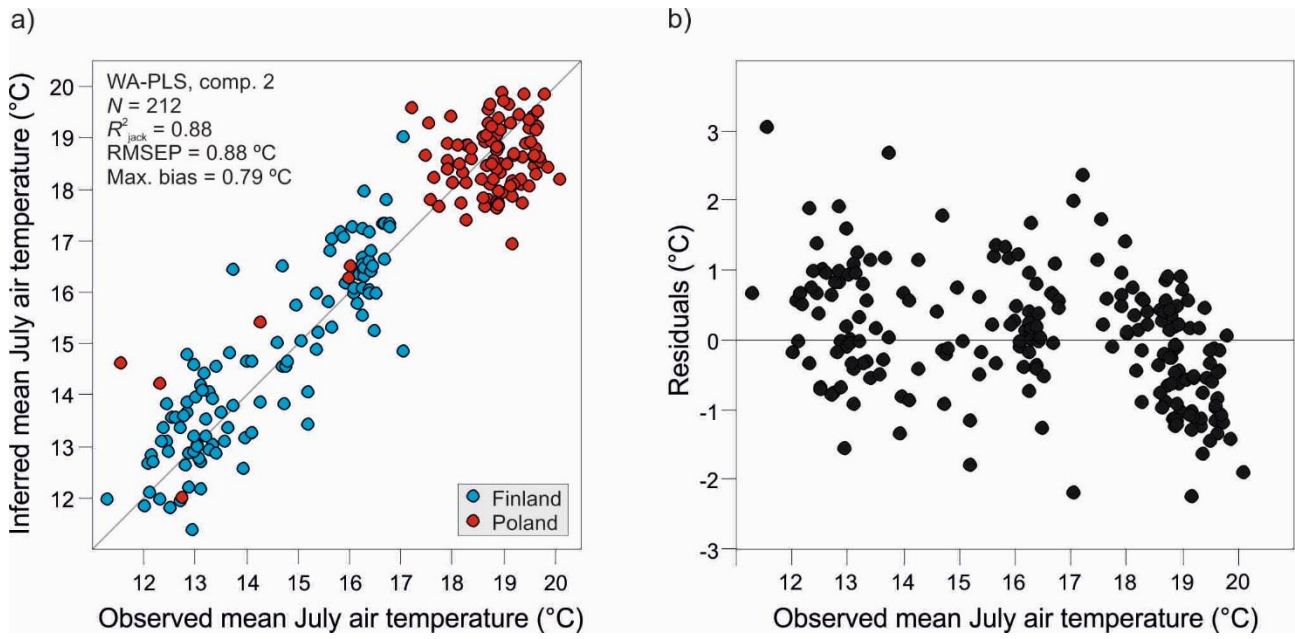
829

830

831

832

833



834

835 Fig. 5. (a) Relationship (1:1) between observed and chironomid-inferred mean July air temperatures  
 836 in the East European calibration model using the Weighted Averaging-Partial Least Squares (WA-  
 837 PLS) technique with two regression calibration components.  $N$  = number of calibration sites,  $R^2_{\text{jack}}$   
 838 = jackknife cross-validated correlation coefficient, RMSEP = root mean squared error of prediction.

839 (b) Residuals versus observed temperatures.

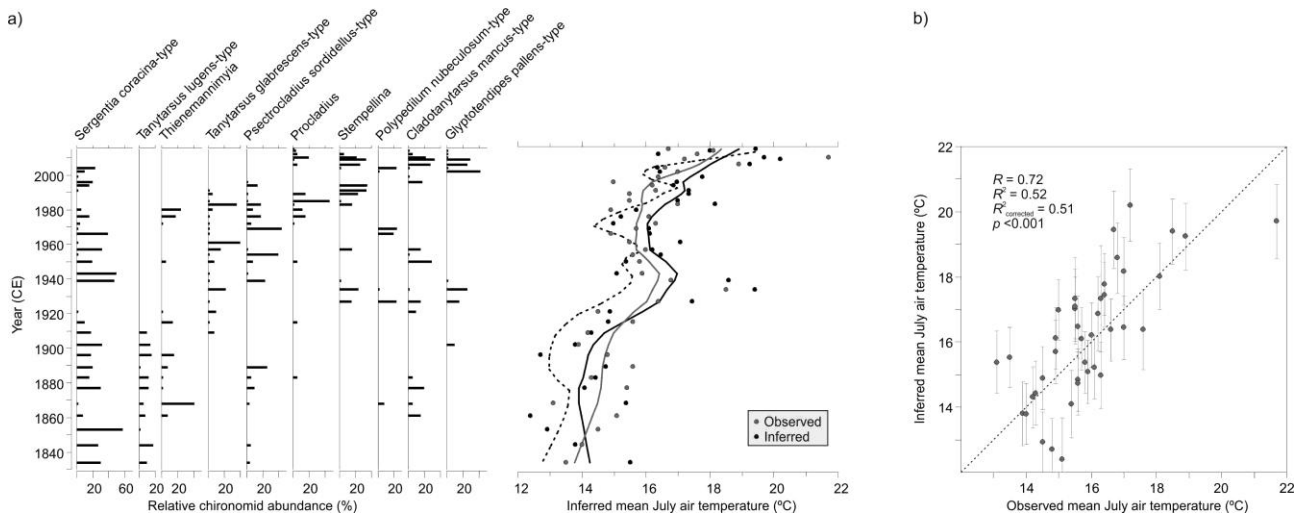
840

841

842

843

844



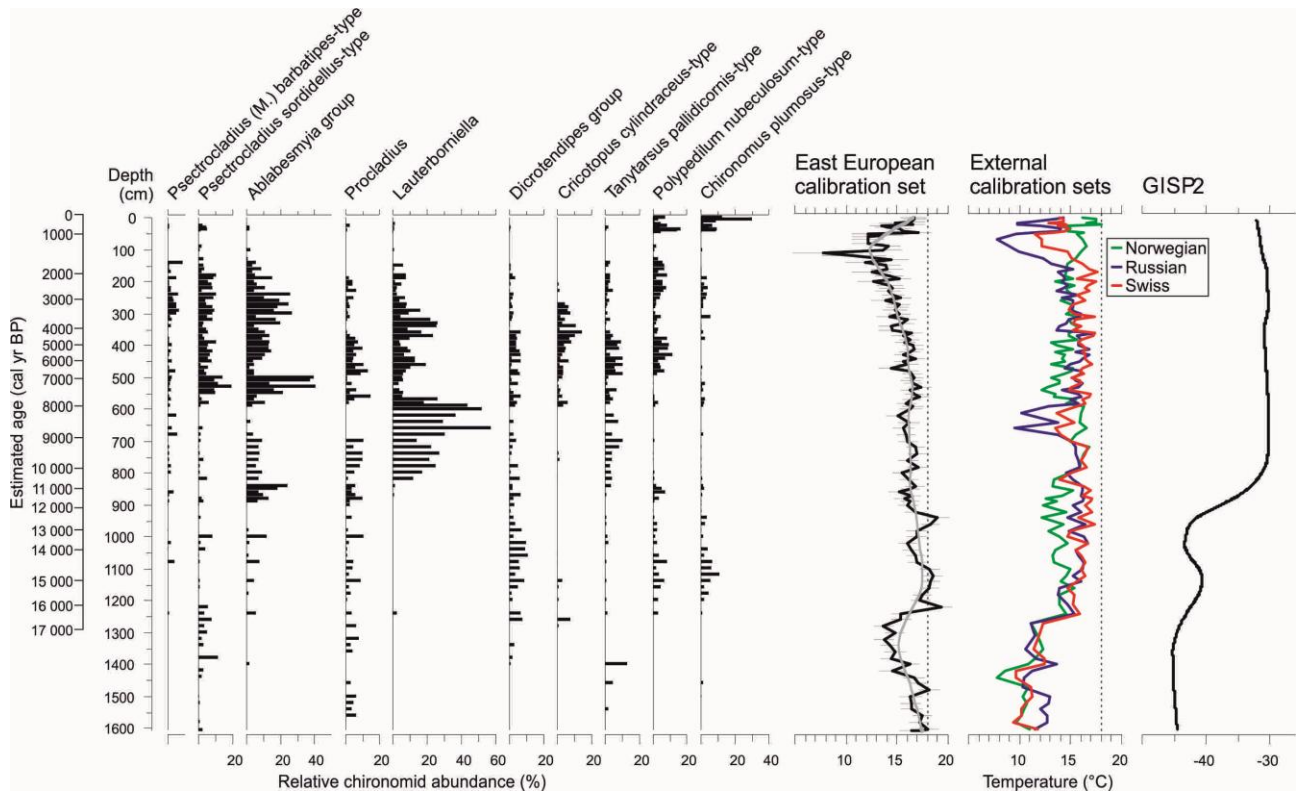
845

846 Fig. 6. Ten most common chironomids (Luoto & Ojala 2017) and chironomid-inferred mean July  
 847 air temperature reconstruction from Lake Nurmijärvi (southern Finland) using the East European  
 848 calibration model compared with instrumentally measured temperatures (a) and their 1:1  
 849 relationship with sample-specific error estimates using bootstrapping cross-validation (b). The  
 850 dashed curve is the smoothed (LOESS span 0.2) original reconstruction using the Finnish model  
 851 (Luoto & Ojala 2017). The taxa are ordered according to their temperature optima in the calibration  
 852 set from the coldest to warmest.

853

854





855

856 Fig. 7. Ten most common chironomids (Płóciennik et al. 2011) and chironomid-inferred mean July  
 857 air temperature reconstruction from Żabieniec paleolake (Poland) using the East European  
 858 calibration model compared with reconstructions (Płóciennik et al. 2011) using the Norwegian,  
 859 Swiss and Russian calibration datasets. The taxa are ordered according to their temperature optima  
 860 in the calibration set from the coldest to warmest. The gray line in the new reconstruction represent  
 861 LOESS smoothing (span 0.2) and the error bars represent the bootstrap estimated sample-specific  
 862 errors. Modern temperature at the study site is drawn as dashed lines. The smoothed (0.2)  
 863 Greenland ice core data (GISP2, Cuffey & Clow 1997; Alley 2000) is provided to illustrate  
 864 hemispheric temperature development (note that the timescale is only tentative due to chronological  
 865 uncertainties).